NANOINDENTATION ON ULTRA HIGH PERFORMANCE CONCRETE SYSTEM

JIŘÍ NĚMEČEK[a]*, CHRISTIAN LEHMANN[b], and PATRICK FONTANA[b]

[a] Czech Technical University in Prague, Thákurova 7, 16629 Prague 6, Czech Republic, [b] BAM Federal Institute for Materials Research and Testing, Unter den Eichen 87, 12205 Berlin, Germany
jiri.nemecek@fsv.cvut.cz

Keywords: mechanical properties, nanoindentation, grid indentation, heterogeneous system, ultra high performance concrete

1. Introduction

In the past decade, nanoindentation has become commonly used experimental technique for obtaining quantitative data on elastic and inelastic material properties in small volumes, typically in submicron length scale. The methodology was developed mainly for homogeneous materials or, at least, the homogeneity is assumed far enough from the tested volume in evaluation procedures[1]. Measurement on a heterogeneous system, in which the material phases are intermixed in small volume, is still a challenging task due to several circumstances. First, the preparation of a flat surface on the heterogeneous sample with high differences in stiffness needs special care. Second, the mechanical interaction between the material phases during surface loading is often unavoidable and therefore the extraction of intrinsic properties of individual phases from the heterogeneous system may not be possible. If differences between the stiffnesses of the interacting phases are low, finding of intrinsic properties can be successful using conventional evaluation[1,2]. In other cases, the error in estimating intrinsic properties can reach tens of percent[3,4].

2. Motivation

Many structural materials which are used or are being developed in the construction show high degree of heterogeneity. Ultra high performance concrete (UHPC) is representing an example of such engineering material with a complex microstructure. Overall mechanical properties of UHPC can be tested by conventional methods. However, some phenomena that are interlinked directly with the microstructure can be disclosed exclusively by small scale methods like nanoindentation. Due to enhanced curing conditions at higher temperature (autoclaving) waste materials like fly ash or slag[5,6] can be added to reduce the amount of Portland cement in UHPC. It was found that after autoclaving the samples show some kind of zoning which is exhibited in optical microscope as lighter outer part and darker inner part. It was supposed that the zoning could be caused by an inhomogeneous autoclaving effect in the matrix which in turn could cause also different mechanical behavior of these parts. The zoning was most pronounced in cases when slag was used in the mixture[6]. This finding led us to the idea of testing mechanical resistance of different parts in the sample by micromechanical method, the nanoindentation.

3. Methodology

In order to evaluate the difference in mechanical performance of different zones in the sample (inner and outer parts) grid nanoindentation was employed. Cross sections of the samples were polished and two arbitrarily chosen areas were selected. One in the inner part of the sample and one in the outer part within 4 mm from the sample edge where the zoning was previously observed.

Selected locations were indented by means of massive grid indentation in order to receive large statistical set of data from all material phases. Large number (200–300) of indents was performed on each sample location and elastic properties were computed for individual imprints. The size of indents was chosen to be small (~200 nm in depth). However, it was not possible to keep the indents' size considerably smaller than that of all neighboring features due to extreme microstructural heterogeneity. Therefore, it was not possible to avoid all phase interactions which must be kept in mind and results introduced afterward have to be taken not as individual phase properties but more or less average mechanical properties of the small material volume around the indents. Regardless the indent location, individual results were analyzed by a standard method[1]. Subsequently, histograms of elastic properties of all measurements were plotted and analyzed by means of statistical deconvolution[2,3,7].

4. Sample preparation

Three types of UHPC mixtures were tested. The proportionally uniform composition of the samples (Tab. I) varied in the type of the secondary cementitious materials, aggregate and filler (Tab. II). The water to cement ratio was 0.31 by weight and superplasticizer was used in all cases.

All samples were autoclaved for 6 hours at 180 °C and 12 bar (water vapor saturation) pressure. Heating and cooling took 1 hour each. It is assumed that almost all hydration takes place during the autoclaving period. Then, samples were stored in ambient conditions. Flat surface suitable for nanoindentation was obtained by mechanical polishing before testing.

Table I
Concentrations of sample components (kg m^{-3})

Cement	Micro-silica	Second-ary mat.	Filler	Aggregate (0-2mm)
760	74	76	248	970

Table II
Sample specification

Sample	Secondary material	Filler	Aggregate (0-2mm)
K1-1	class F fly ash	quartz	quartz sand
K1-2	granulated blast furnace slag	quartz	quartz sand
K2-1	class F fly ash	quartz	basaltic sand

5. Measurement

Since matrix properties were of prior interest, indentation locations were selected not to contain large pores or large grains of aggregate. Each location was covered by a rectangular grid of indents with 15 μm spacing in both directions. Maximum indents' depth was prescribed ~200 nm. Loading diagram contained linear loading 24 mN min^{-1}, holding period at the peak for 10 s and linear unloading 24 mN min^{-1}. The insertion of the holding period, in which material creep is demonstrated, is important for unbiasing the unloading stage in case of testing inelastic material[8].

Optical observations showed on the microstructural complexity as illustrated in Figs 1 and 2.

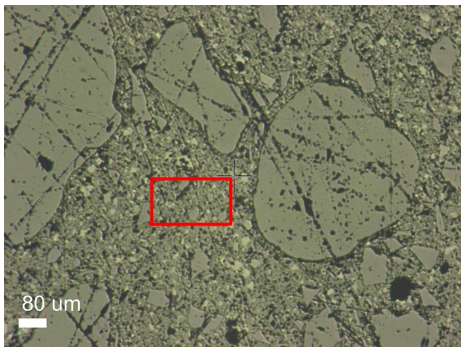

Fig. 1. **Example of the sample microstructure and grid location in the outer zone of sample K1-2**

6. Results

As it was mentioned above, even if the indentation depth was low (~200 nm) it was not possible to avoid interference of the distinct phases in the material due to very high heterogeneity and phase mix. Therefore, the following micromechanical results have to be considered as effective properties of the phase compound within the affected volume. This volume can be estimated as three times maximum depth[2], i.e. ~600 nm.

First, elastic modulus (E) and hardness (H) were evaluated for individual indents[1] using the assumption of constant Poisson's ratio ν=0.2 for all samples. It was found that both elastic modulus and hardness exhibit very similar distributions. Therefore, elastic modulus was used preferably in the following. Maps of E were plotted over the tested area to show on high heterogeneity and representativeness of the selected areas which contain all possible mechanical phases from low to high stiffness (Fig. 3).

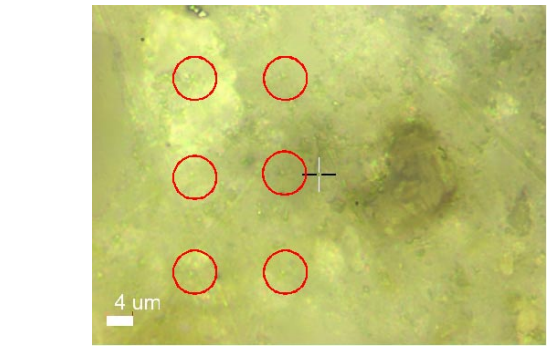

Fig. 2. **Part of the indentation grid in the outer zone of sample K1-2 (slightly visible individual indents are circled)**

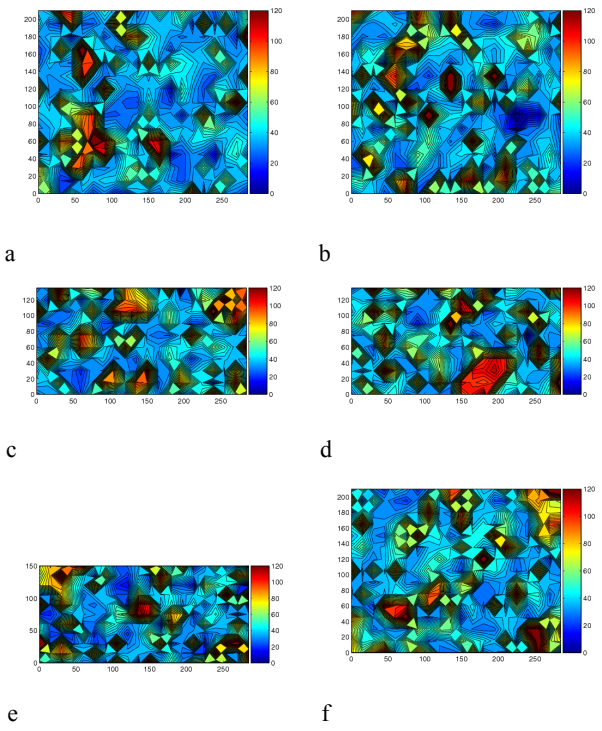

Fig. 3. **Maps of elastic moduli (GPa) over tested areas in a sample inner part (left) and outer part (right). (a-b) belongs to K1-1, (c-d) to K1-2 and (e-f) to K2-1**

Second, loading diagrams (depth-load curves) showed high variation due to the heterogeneity. Therefore, it is reasonable to evaluate the results in the form of histograms of all received parameters which show on the distribution of mechanical phases over the representative areas. Several peaks with high frequency of occurrence could be distinguished (Fig. 4). Afterwards, histograms were plotted in one graph to see the differences between the samples (Fig. 5).

It can be seen in Fig. 5 that all histograms are very similar which shows on similar mechanical behavior of all samples and phases in it. Frequency of occurrence varies a bit. More exact comparison is given by the following deconvolution.

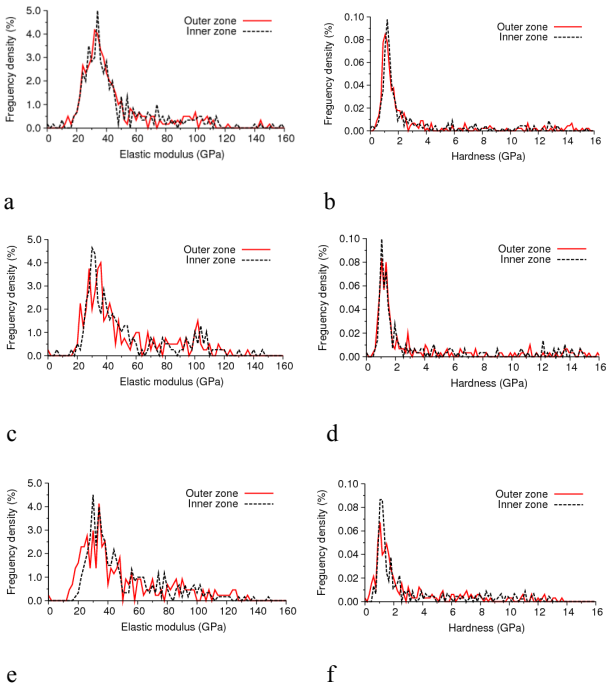

Fig. 4. **Histograms of elastic moduli (left) and hardness (right). (a-b) belongs to K1-1, (c-d) to K1-2 and (e-f) to K2-1**

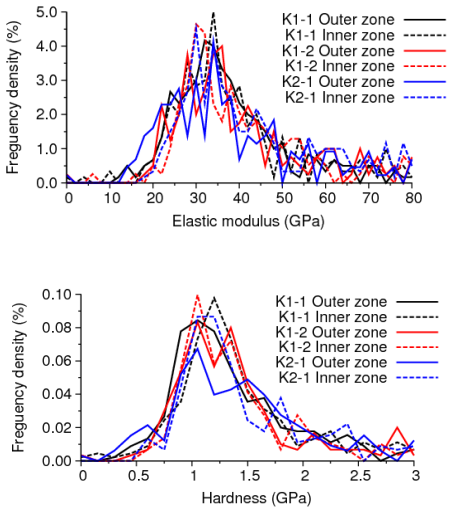

Fig. 5. **Histograms of elastic moduli (top) and hardness (bottom) for all tested locations**

Finally, the histograms of elastic moduli were analyzed by the deconvolution algorithm[2,3,7] in order to separate the overall distribution (whole histogram) into two individual phases. It is supposed that the first phase contains all lower stiffness phases (products of hydration after autoclaving). The second phase contains all the rest, i.e. unhydrated clinkers, quartz, non-reacted fly-ash and other high stiffness phases. It could be possible to perform deconvolution into more than two phases but for the sake of simplicity and clear comparison between the samples, only two (one dominant and the rest) were assumed (see Fig. 6).

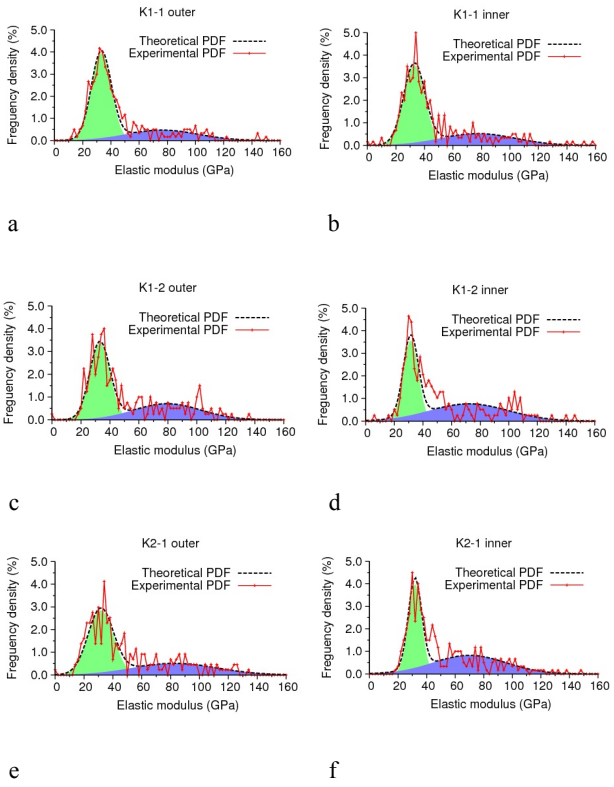

Fig. 6. **Deconvolution of the overall distribution into two individual phases. (a-b) belongs to K1-1, (c-d) to K1-2 and (e-f) to K2-1**

The deconvolution was based on the algorithm[2,3,7] which seeks for n-Gauss distributions in an experimental probability density function (PDF). Random seed and minimizing criteria of the differences between the experimental and theoretical overall PDFs are computed in the algorithm to find the best fit. Table III contains numerical results from the deconvolution also with the estimated volume fractions of the phases.

The first, major phase is characterized with a very similar E~31–33 GPa for all samples and all positions. Therefore, the hypothesis of different mechanical behavior of inner and outer parts in case of slag containing samples (K1-2) was not confirmed. Although the difference in E between the parts was the highest for K1-2 sample, it was still within 5% which is considered to be irrelevant. Volume fractions varied a bit. Higher frequency of the lower stiffness phase was found for

K1-1 and a bit lower for K1-2 and K2-1.Perhaps, it is dependent mainly on the location indented which can contain more or less unreacted material or aggregate. The second phase contains results from all other (higher stiffness) material components and thus the deviation from the mean is high in this case (Tab. III).

Table III
Results of the deconvolution into two phases

	First phase E_1 (GPa)	vol. %	Second phase E_2 (GPa)	vol. %
K1-1 outer	33.20±7.05	69.7	76.25±25.39	30.3
K1-1 inner	32.90±7.45	66.3	77.57±26.00	33.7
K1-2 outer*	33.07±7.00	59.0	79.58±23.15	41.0
K1-2 inner*	31.52±5.22	46.9	72.12±27.73	53.1
K2-1 outer	31.61±8.75	62.4	82.75±29.37	37.6
K2-1 inner	31.81±4.69	47.0	69.93±25.60	53.0

Note: * asterisk denotes slag containing samples K1-2.

7. Conclusions

A very complex microstructure of UHPC samples was studied by means of grid nanoindentation and statistical deconvolution methods. This methodology gives access to the separation of the wide variety of results from this heterogeneous system into limited number of mechanical phases. In this work, differences between the samples and their regions (inner and outer) were studied based on two phase separation. Following major conclusions could be deduced.

- It was found that both elastic modulus (E) and hardness (H) have very similar distributions for reacted parts of the matrix of all samples and all positions with no significant differences between outer and inner parts. The difference in E was found to be within 5%.
- Material properties of unreacted parts and aggregate are also similar for all samples. Their volume fractions are influenced by the selected location for indentation which could contain more or less of these phases.
- Based on low magnification optical images it can be seen that samples contain large amount of porosity. This "large or capillary" porosity is not included in the results and indents laid between the pores. So, if there is some effect of porosity on the overall stiffness or strength of the matrix, this could not be disclosed by nanoindentation.

Finally, it can be concluded that there is probably no significant difference in the mechanical behavior of the sample matrices. Therefore, any differences between the outer and inner parts in terms of their overall stiffness or strength can be caused by different capillary porosity or other effects but the stiffness of the cementitious matrix and their components.

Support of the Czech Science Foundation (GA ČR 103/09/1748) and Ministry of Education of the Czech Republic (MSM 6840770003) is gratefully acknowledged.

REFERENCES

1. Oliver W., Pharr G.: J. Mat. Res. *7* (1992).
2. Constantinides G., Chandran K. R., Ulm F.-J., Vliet K. V.: J. Mater. Sci. Eng., A *430* (2006).
3. Němeček J., Lukeš J.: Chem. Listy *104*, s279 (2010).
4. Kabele P., Davydov D., Jůn P., Němeček J., Jirásek M.: *Proceedings of Concreep 2008*.
5. Lehmann, C., Müller, U., Fontana, P.: *Proceedings of NICOM3, 2009*, 287–293.
6. Fontana P., Lehmann C., Müller U., Meng B.: *Proc. Int. RILEM Conference on Material Science (MatSci), 2010*, Vol. III, 69–77.
7. Němeček J., Šmilauer V., Kopecký L., accepted for publication in Cem. & Concr. Comp., ISSN: 0958-9465.
8. Němeček J.: Mater. Character. *60*, 1028 (2009).

J. Němeček[a], Ch. Lehmann[b], and P. Fontana[b] *([a] Czech Technical University in Prague, Faculty of Civil Engineering, Czech Republic, [b] BAM Federal Institute for Materials Research and Testing, Division "Building Materials", Germany):* **Nanoindentation on Ultra High Performance Concrete**

The paper describes results from nanoindentation on a very heterogeneous structural material, namely ultra high performace concrete (UHPC). Nanoindentation was used to investigate the influence of mixture components and production conditions on the mechanical response of the hydrated matrix after autoclaving. Statistical grid nanoindentation complemented with the deconvolution procedure revealed that the matrix properties of all tested mixtures are very similar without any significant difference in their stiffness or elasticity, respectively.

It is assumed that the sample zoning after autoclaving, which is exhibited in optical microscopy as different color of inner and outer parts, is caused by secondary effects like increased porosity.

MODELLING OF HARDNESS DISTRIBUTION CURVES OBTAINED ON TWO-PHASE MATERIALS BY GRID INDENTATION TECHNIQUE

JIŘÍ BURŠÍK

Institute of Physics of Materials, Academy of Sciences of the Czech Republic, Žižkova 22, 61662 Brno, Czech Republic
bursik@ipm.cz

Keywords: grid indentation, hardness, modelling

1. Introduction

Multiphase materials with fine microstructural features (secondary phase particles, grains of different phases, inclusions, voids, etc.) are challenging for obtaining sound and accurate mechanical characteristics of individual phases. Current advances of instrumented indentation techniques[1] provide the way of measuring the mechanical response of individual phases at the length scale of 10^{-6} m with nanoindenters and even below that with dedicated AFM devices or special sample holders[2] for *in-situ* TEM probing. It is now well established that the response of a material upon the reversal of contact loading provides access to the mechanical properties of the indented material[3].

In the field of instrumented indentation experiments, the so called grid indentation technique (GIT) was proposed[4,5], which consists in making a large array of micro to nanoscale contact experiments and the statistical analysis of the resulting data. GIT uses the advantage of high level of automation of today's nanoindentation instruments; the number of indents in the regular grid is typically of the order of hundreds to thousands[6]. The technique can be conveniently used for heterogeneous materials; however, the proper choice of parameters of the indentation experiment is crucial and critical.

Considering a characteristic size D of structural objects and an indentation depth h, two limiting cases can be identified (Fig. 1). For $h>>D$, the average properties of the composite material are obtained. If $h<<D$, a single indentation test yields properties of the particular constituent phase under indenter. In this case the data allow also the evaluation of volume fraction of constituent phases and construction of 2D maps of the measured mechanical properties. The usual way of processing the frequency distribution curves of mechanical properties obtained by GIT is the multimodal Gaussian fitting[5–7]. The latter limiting case (i.e. $h<<D$) is more rewarding but also more difficult to reach. In practice we can hardly avoid all the phase interfaces and other structural features causing a departure from single phase values and the actual results are often situated in some intermediate state between the two limiting cases.

In this work, the hardness distribution curves obtained by GIT are computer modelled for various volume fractions of spherical particles and for the wide range of indentation loads covering also the intermediate states of possible GIT outputs. The effect of the input parameters on the distribution curves is discussed and potential pitfalls of the routine statistical evaluation by multimodal Gaussian fit are examined.

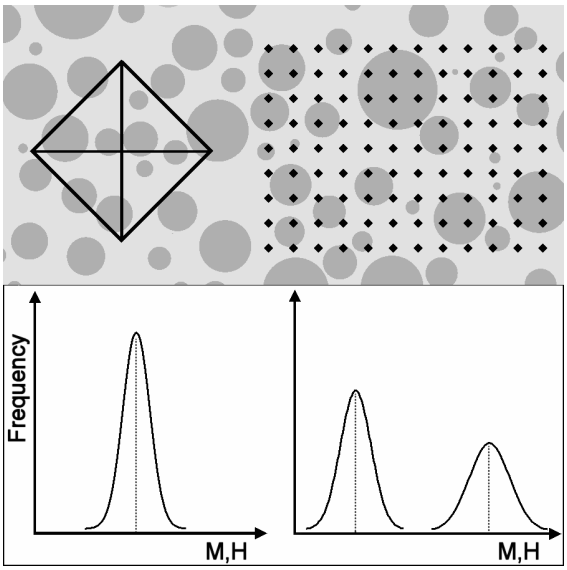

Fig. 1. **The principle of the grid indentation technique for heterogeneous materials and the scheme of the two limiting cases. Large indentation depths (left) lead to the response of the homogenized medium. Small indentation depths (right) allow the evaluation of properties of individual constituents. Horizontal axis most often represents either indentation modulus *M* or indentation hardness *H***

2. Model details

The tested material was modelled as a cube (edge size 1000 arbitrary units) filled with spherical particles. Periodic boundary conditions and log-normal distribution of particle diameters with the median exp(μ)=55 a.u. and the standard deviation σ=0.4 were used (Fig. 2). For three selected levels of particle volume fraction (10, 40 and 60 %), there were 583, 2331 and 3496 particles in the cube, respectively.

Parameters of the two phases were chosen to represent hard particles (p) in a soft matrix (m), namely elastic moduli E_p=380 GPa, E_m=200 GPa, yield points Y_p=8000 MPa, Y_m=667 MPa, Poisson ratios $\nu_p=\nu_m$=0.3. Hardness of the phases was described as

$$H = 3Y \qquad (1)$$

thus making H_p=24 GPa and H_m=2 GPa. Contact radius under indenter a was described as the half-diagonal of the Vickers indentation:

$$a = \sqrt{\frac{1.854P}{4H}} \qquad (2)$$

where P is an applied load. The plastic zone radius c was evaluated according to Johnson's model[8] as

$$c = a\left[\frac{E\tan\beta}{6Y(1-\nu)} + \frac{2}{3}\left(\frac{1-2\nu}{1-\nu}\right)\right]^{1/3} \quad (3)$$

where β is the angle between the indenter flank and the sample surface (22 deg for Vickers tip). The *c*-*P* relation is shown for both phases in Fig. 3.

The graph shows the broad range of applied loads and plastic zone radii used for simulations. The *P* axis scales according to the 'arbitrary unit' of length in the simulation (cube size, particle diameters, plastic zone radius): e.g. if a.u.=nm (resp. mm), the load axis in Fig. 3 scales in μN (resp. N).

The plastic zone volume was adjusted according to the phases under indenter and then the hardness was calculated according to the mixing law proposed by Burnett and Rickerby[9,10]:

$$H = f_p H_p + f_m H_m \quad (4)$$

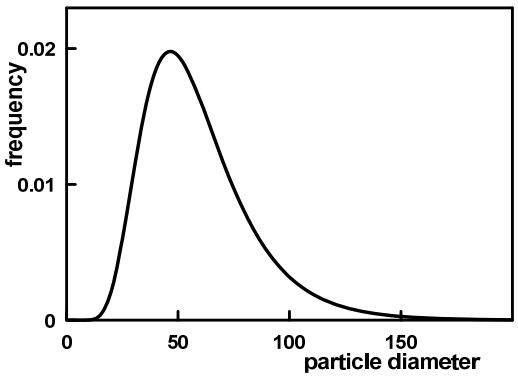

Fig. 2. **The log-normal distribution of particles randomly placed in the modelled cubic block**

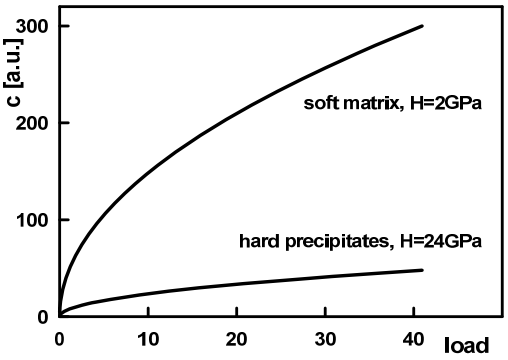

Fig. 3. **The plastic zone radius as depending on the indentation load**

where f_p and f_m are the volume fractions of the phases in the hemispherical plastic zone under the indenter tip. A regular grid of 100×100×100 points was used to simulate the hardness frequency distribution curves (meaning making a 100×100 grid at the cube face, then removing the thin slice and repeating the sequence down the whole cube).

It should be noted that many important practical details of the real indentation process are not dealt with in this model (such as surface roughness, realistic tip geometry, specific material response etc.) and it is focused mainly on the behaviour of hardness frequency distribution curves obtained by grid indentation.

3. Results and discussion

The effect of increasing indentation load is demonstrated on hardness maps in Fig. 4.

Many small particles are averaged out in the map produced at high load. Only inner cores of the large particles retain the true characteristics of the hard phase.

From a series of simulated hardness distributions, several curves were selected to illustrate and discuss important features. In general, the peak of the soft phase is more prone to various artifacts as the plastic zone is larger in soft places and hence the measured value of hardness is more affected by various perturbations in the indentation vicinity.

Starting from the limiting case of the two distinguished peaks of the soft and the hard phase, the first change observed with gradually increasing load is the increasing counts in the right-hand branch of the soft phase peak (Fig. 5).

The peaks still represent well the correct single phase values. However, in practice the grid indentation experiments provide us with typically 10^2 to 10^3 points and the histograms

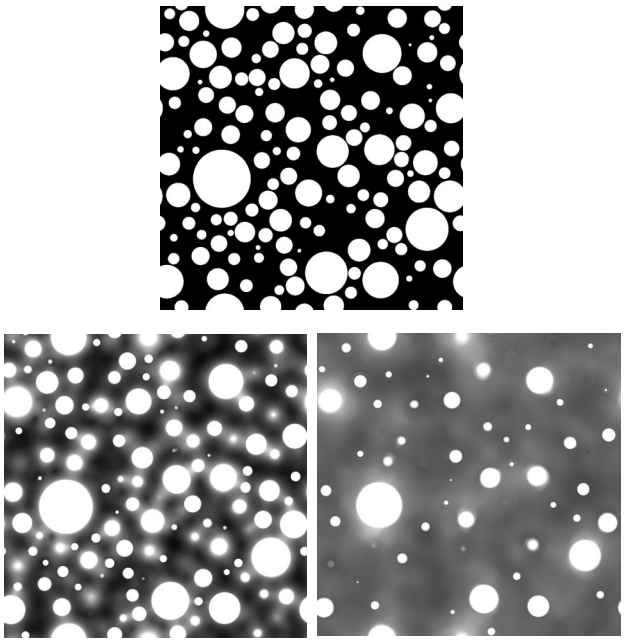

Fig. 4. **The phase map of 40 vol. % sample and two hardness maps produced at medium (*P*=1.37) and high (*P*=10.6) load**

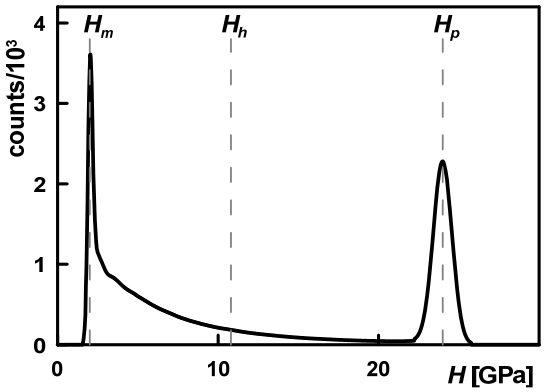

Fig. 5. **The hardness histogram obtained using the load *P*=0.18 a.u. on the model with 40 vol.% of particles.** Dashed vertical lines denote the hardness values of single phases H_m and H_p and the hardness of homogenized medium H_h

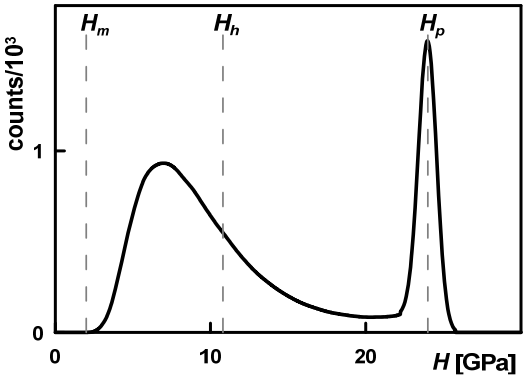

Fig. 6. **The hardness histogram obtained using the load of *P*=1.38 a.u. on the model with 40 vol.% of particles**

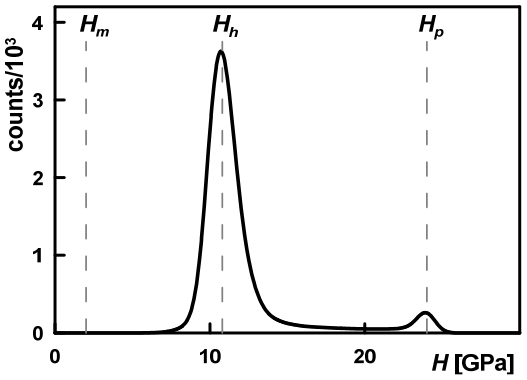

Fig. 7. **The hardness histogram obtained using the load of *P*=18.2 a.u. on the model with 40 vol.% of particles**

are more fuzzy, without clear depiction of the shape (for comparison: 10^6 grid points were used for the modelled histogram in Fig. 5), hence we cannot rely on 'seeing' the correct soft phase peak position. If we attempt to fit the left part of the histogram by a symmetric Gaussian curve, then its mean value is always systematically shifted from the correct peak position to higher values. As a matter of fact, as soon as we leave the ideal case of hitting only single phase regions, the soft phase peak loses its symmetry and fitting it by a symmetric Gaussian curve is questionable.

Further load increase causes the soft phase peak to 'transfuse' into an intermediate peak that gradually shifts across the region between H_m and the hardness of homogenized medium H_h (Fig. 6). The position of the intermediate peak depends on the applied load and does not provide any information about H_m. However, the operator may be mislead by the overall shape of the histogram in Fig. 6 and use the left peak for fitting and evaluation of the soft phase hardness (and perhaps also for the evaluation of the volume fraction). To avoid this pitfall, the hardness distribution curves should be measured at several loads and peak position stability should be checked for.

Yet further load increase causes a distinctive lowering of the hard phase peak and further growth of the intermediate peak. The shifting of the intermediate peak slows down and finally stops at the homogenized medium hardness H_h (Fig. 7.)

Histogram series obtained on materials with 10 and 60 vol.% of particles gave qualitatively similar results. The main quantitative differences were naturally the peak heights and the value of H_h. Another quantitative difference consists in the load values characteristic of various stages depicted in the previous graphs (Fig. 5–7): the characteristic loads are shifted towards higher values for 10 vol.% and in the opposite direction for 60 vol.%.

One more feature worth mentioning was found in a narrow range of loads situated between the cases described in Fig. 5 and Fig. 6, where the soft phase peak is still visible and the intermediate peak is of comparable height. In a result the histograms temporarily show three peaks for a two-phase material (Fig. 8).

Overview of the hardness distribution curves hence offers a rather pessimistic view of the utilization of the grid indentation technique for obtaining characteristics of individual phases beyond the limit $h<<D$: unless the limit is fulfilled (and is it ever, taking into account that h cannot be arbitrarily small due to limitations imposed by both the instrument and the sample?), we cannot rely on the symmetry and/or position of some peaks and even the number of peaks is not always representative of the number of phases.

4. Summary

The hardness distribution curves obtained by grid indentation technique were computer modelled for various volume fractions of spherical particles and a range of indentation loads using a simplified description of the indentation event. The effect of various parameters on the distribution curves

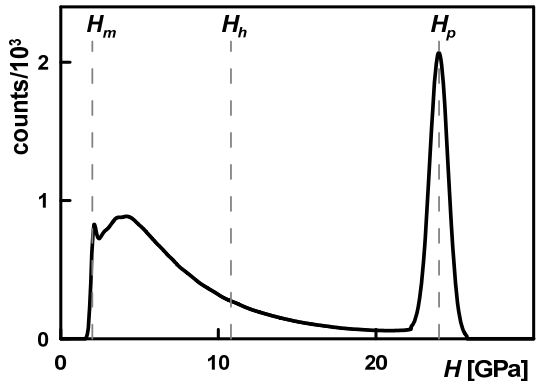

Fig. 8. **The hardness histogram obtained using the load *P*=0.41 a.u. on the model with 40 vol. % of particles**

was discussed and potential pitfalls of their routine statistical evaluation by multimodal Gaussian fit were examined.

The financial support for this work was provided by the Czech Science Foundation (Project 106/09/0700). Vilma Buršíková is acknowledged for stimulating discussions.

REFERENCES

1. Fischer-Cripps A. C.: *Nanoindentation*, Springer Verlag, New York 2003.
2. http://www.nanofactory.com
3. Oliver W. C., Pharr G. M.: J. Mater. Res. *19*, 3 (2004).
4. Constantinides G., Ravi Chandran K. S., Ulm F. J., Van Vliet K. J.: Mater. Sci. Eng., A *430*, 189 (2006).
5. Constantinides G., Ulm F. J.: J. Mech. Phys. Solids *55*, 64 (2007).
6. Randal N. X., Vandamme M., Ulm F. J.: J. Mater. Res. *24*, 679 (2009).
7. Němeček J., Lukeš J.: Chem. Listy *104*, 279 (2010).
8. Johnson K. L.: J. Mech. Phys. Solids *18*, 115 (1970).
9. Burnett P. J., Rickerby D. S.: Thin Solid Films *148*, 41 (1987).
10. Burnett P. J., Rickerby D. S.: Thin Solid Films *148*, 51 (1987).

J. Buršík *(Institute of Physics of Materials, Academy of Sciences of the Czech Republic, Brno):* **Modelling of Hardness Distribution Curves Obtained on Two-Phase Materials by Grid Indentation Technique**

While using a grid indentation technique on a multiphase material, we are often situated somewhere between the two limits of the method, i.e. between obtaining the true material properties of individual constituent phases and obtaining the averaged properties of a composite material. In this work, the hardness distribution curves obtained by the grid indentation technique are computer modelled for various volume fractions of spherical particles, range of indentation loads and various mechanical properties of constituent phases. The effect of these parameters on the distribution curves is discussed and potential pitfalls of their routine statistical evaluation by multimodal Gaussian fit are examined.

MECHANICAL PROPERTIES OF HARD PARTICLES IN SOFT MATRIX

PAVOL ZUBKO[a]*, LADISLAV PEŠEK[a], OLGA BLÁHOVÁ[b]

[a] Technical university of Košice, Department of materials science, Letná 9, Košice, Slovakia, [b] Universtiy of West Bohemia, New Technology Research Center, Plzeň, Univerzitní 8, Czech Republic
pavol.zubko@tuke.sk

Keywords: Hard particles, soft matrix, inclusion, IF steel

1. Introduction

According to recent studies FE (Finite Element) analysis allows us to simulate behaviour of components and materials before their physical existence[1]. For good FE model we need to learn about the properties of all phases and describe how they affect the global properties.

In steels we can find particles, except the mayor phase, which affect the final properties of materials. Hard particles usually delaminate from matrix under loading, soft particles crack. In both cases knowledge of properties of particles are important to correct simulation of material behaviour.

Nanoindentation is a powerful tool to determine mechanical properties in small regions, phases, objects and particles, too.

The aim of the contribution is to determine mechanical properties of particles in an IF steel and to evaluate the influences affecting the precition of the nanoindentation measurement of hard particle in the soft matrix.

2. Experimental material

An interstitial free steel (IF) was used for experiments. In this steel all interstitial elements are bound in the form of stabile inclusions. For purpose of this contribution it will be called the particles. Chemical composition of the investigated steel is in Tab. I.

Table I
Chemical composition of investigated IF steel

C [%]	Mn [%]	Si [%]	P [%]	S [%]	Al [%]	Ti [%]
0.005	0.145	0.0128	0.006	0.006	0.042	0.064

Ferrite polyhedric grains and particles were found in the microstructure, Fig. 1. The particles were identified as TiC(N) particles by the EDX analysis. Size distribution of particles is shown in Fig. 2 and Tab. II.

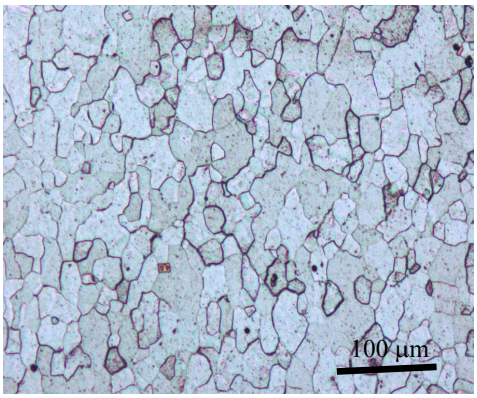

Fig. 1. **Microstructure of investigated IF steel**

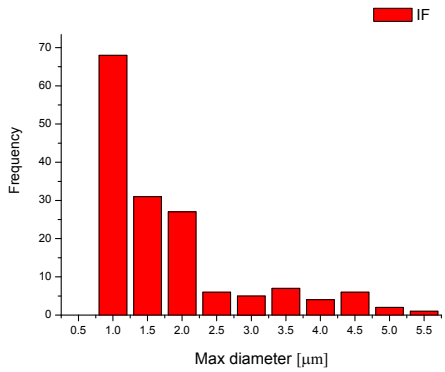

Fig. 2. **Histogram of size distribution of investigated particles**

Table II
Average size of investigated IF steel particles

	Mean diameter [µm]	Perimeter [µm]	Max length [µm]	Area [µm^2]	No.
IF	1.55	3.47	2.05	2.24	158

3. Experimental equipment

First experiments were performed using Shimadzu DUH202 instrument equipped with a Vickers tip[2]. DUH202 is an older equipment and measurements are connected with problems as correct processing of data, which are not affected by first contact selection; area function, thermal drift, etc.

Nevertheless, the data of hardness and Young modulus were measured, Tab. III.

Table III
Average Hardness and Modulus values of IF matrix and particles

	H_{IT} [GPa]	E_{IT} [GPa]
Matrix	1.40±0.12	200±14
TiC(N) particles	5.75±0.49	266±22

Matrix hardness and modulus values are according the literature[3] but TiC(N) particles hardness and modulus values were expected to be double[4,5].

Next experiments were performed using the Nanoindeter XP equipped with a Berkovich tip with rounding ~ 20 nm. Ten measurements in continues stiffness mode were performed on selected particles to the indentation depth of 1 μm. One indent was performed on each particle. Samples for experiments were prepared metallographically.

4. Reusults and discussion

Indentation hardness (H_{IT}), Young modulus (E_{IT}) in relation to indentation depth were monitored (Fig. 4 and Fig. 6). Curves were evaluated by the following way: in area of the peak region a part of curve was determined where the values of hardness and modulus are relatively constant. Values of hardness, modulus, depth and corresponding force together with position of indent after indentation were evaluated for this curve. Results are presented in the Tab. IV. On indentation curves (F-h) were observed changes of loading trend (Fig. 3) and pop-ins (Fig. 5). Those artefacts are connected with delamination of particle-matrix interface, impressing of particle into matrix, cracking of particle etc[6].

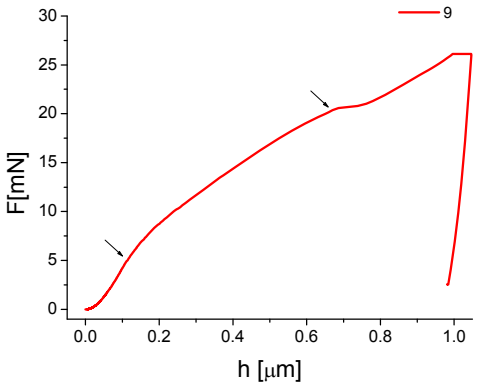

Fig. 3. **Indentation curve of particle no. 9 and particle after indentation**

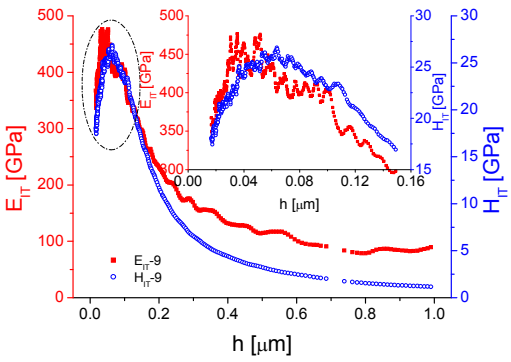

Fig. 4. **Hardness and modulus in relation with indentation depth of particle no. 9**

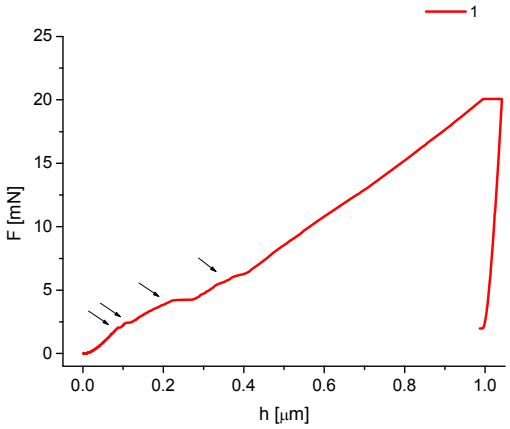

Fig. 5. **Indentation curve of particle no. 1 and particle after indentation**

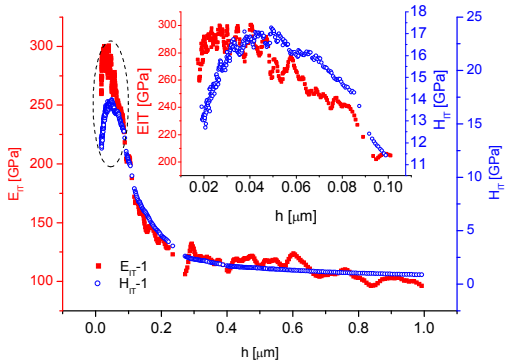

Fig. 6. **Hardness and modulus in relation with indentation depth of particle no. 1**

Table IV
Properties of investigated TiC(N) objects, depth (h) and corresponding force (F) from which were determined values of H_{IT} and E_{IT}, respectively, max perpendicular particle dimesion in the observed plane – b, c

No	H_{IT} [GPa]	E_{IT} [GPa]	h [nm]	F [mN]	b [μm]	c [μm]	Note
1	17	300	20–50	0.3–0.9	3	3	P
2	20	373	30–80	0.6–2.3	3	2	P
3	7	275	10–20	0.05–0.1	5	4	I
4	11	275	15–20	0.07–0.1	3	2	I
5	7	260	30–50	0.4–0.2	4	2	I
6	2	225	300–400	2.3–5.5	5	2	M
7	18	350	30–50	0.5–0.9	4	3	P
8	21	360	20–70	0.2–1.5	9	9	P
9	26	460	30–70	0.2–2.1	4	2	P
10	8	220	70–120	0.7–2.1	4	1	I

P – particle, I – interface, M – matrix

Shape and size of the particle underneath the surface is unknown and depends on basic shape of the particle, on orientation and from its cuts. Finally, effective diameter of particles which resist penetration of indenter is unknown. Results presented in the Tab. IV are with high scatter and are on one side close to matrix values and on other side close to hard TiC (N) coatings. What is correct? What affects the results? One of the many possible influences is impressing of the particle during the indentation into the matrix. If the particle is impressed into the matrix then measured depth (h) is composed from:

$$h = h_i + h_h \qquad (1)$$

indentation depht of the particle into the matrix (h_i) and indentation depth of indenter into the particles (h_h). Suppose that the effective radius of the particle is big enough and the particle is impressed into the matrix only elastically. Indentation of the tip into the particle (h_h) is elasto-plastic :

$$h = h_{ie} + h_{he} + h_{hp} \qquad (2)$$

After expressing[7] the eq. (2) we can achieve following equation:

$$h = \frac{F}{2aE_{rm}} + \sqrt{F}\left(\left(\varepsilon\frac{\sqrt{H_c\pi}}{2E_{rc}}\right) + \left(3\sqrt{3}H_c\tan^2\theta\right)^{-\frac{1}{2}}\right) \qquad (3)$$

In eq. (*3*) there are three unknown parameters: particle hardness (H_c), particle reduced modulus (E_{rc}) and effective radius (*a*) of the particle. An iterative process was used to determine these parameters with following conditions: Iterations were done on all particle measurements, the particles have the same hardness and modulus, radius of the particle can not exceed maximal length of the particle, the cylindrical shape of the particle. The fitting was started at contact point and stopped at first inhomogeneity (pop-in, bending, etc.) on F-h curve. The correctness of eq. (*3*) without particle behaviour term was tested on three different bulk materials, Fig. 7. Calculated and measured data for all three materials are in good agreement.

In Fig. 8, 9 results of simulation using the eq. no (*3*) are presented. Squares symbolize measured curves, dashed lines are simulation of indentation into a bulk material with properties of the particle, solid lines are simulation by the eq. (*3*). The difference between the solid and dashed line describes influence of the particle penetration into the matrix. If this difference is evaluated as stiffness change in relation to reciprocal value of effective radius, it can be seen that relation is linear, Fig. 10. It means that results are strongly influenced by impressing of the particle into the matrix. The influence of the particle size on hardness and modulus values is presented in Fig. 11. The properties measured on the biggest particles could be supposed as the most realistic values and are 30 GPa and 480 GPa for hardness and modulus values, respectively.

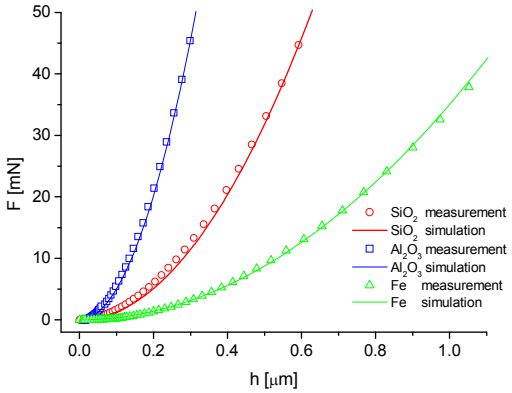

Fig. 7. **Comparison of measurements on bulk materials and simulation by eq. (*3*) without the particle element**

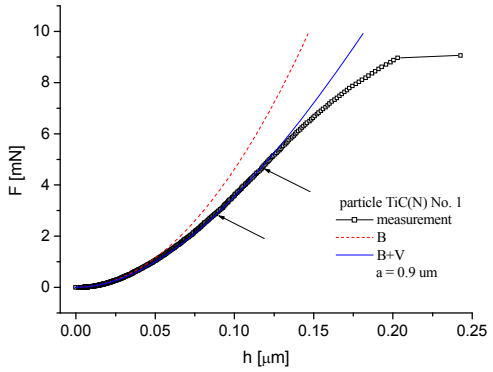

Fig. 8. **Indentation curve of particle no. 9, simulation of bulk material with properties of particle (B) and indented particle (B+V)**

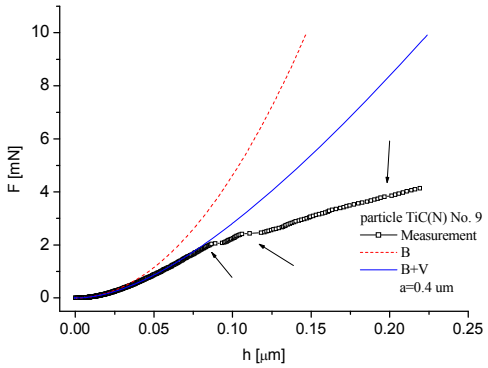

Fig. 9. **Indentation curve of particle no. 9, simulation of bulk material with properties of particle (B) and indented particle (B+V)**

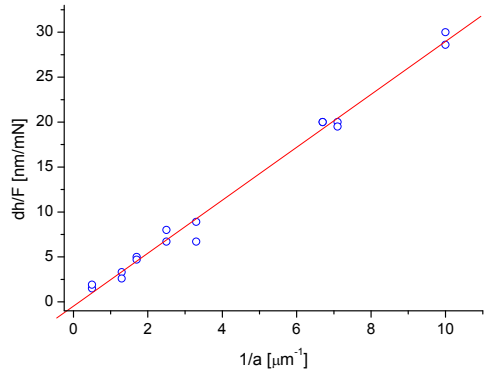

Fig. 10. **Relation between reciprocal value of effective particle radius and stiffness**

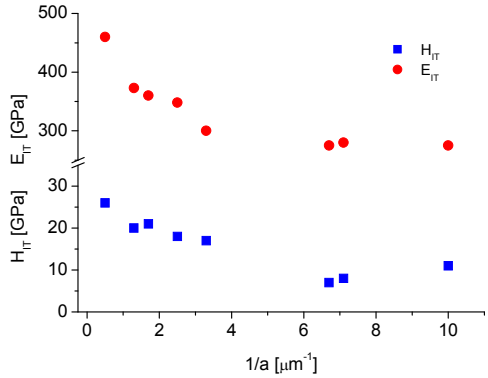

Fig. 11. **Influence of particle effective radius on measured values of hardness and modulus**

5. Conclusions

Following results were obtained from the research presented in this contribution:

– Using DSI method we were able to determine properties of the TiC(N) particles.
– The strong effect of impressing the particles into the matrix during indentation was confirmed.
– The hardness and modulus values of TiC(N) particles are 30 GPa and 480 GPa, respectively.

This work was supported by the grant APVV-0326-07, SK-PL-0019-09, VEGA 1/0846/09.

REFERENCES

1. Mishnaevsky L.: In: *Virtual testing of microstructures as a basis for the optimization of materials*, p. 5–10, IMWF Darmstadt, 2005.
2. Zubko P., Pešek L.: *Fractography of inclusion fractures in deep drawing IF steels. In: Fractography 2003*, (in. Slovak)
3. Tasan C. C., et al.: Acta Mater. *57*, 4957 (2009).
4. An J., Zhang Q. Y.: Surf. Coat. Technol. *200*, 2451 (2005).
5. Hagarová M., et al.: *The Assessment of Properties of PVD Coatings Deposited by ARC and LARC Technology* (in slovak), *In: Vrstvy a povlaky 2009.* Trenčín, Digital Grafhic, 2009.
6. Stus N. V., et al.: J. Alloys Compd. *403*, 305 (2005).
7. Zubko P.: Local mechanical properties in microvolume dimensions of metal materials, *PhD. thesis*, 2008, Košice, in Slovak.

P. Zubko[a], L. Pešek[a], O. Bláhová[b] *([a] Technical university of Košice, Faculty of metallurgy, Department of materials science, Košice, Slovakia, [b] Universtiy of West Bohemia, New Technology Research Center, Plzeň, Czech Republic):* **Mechanical Properties of Hard Particles in Soft Matrix**

The contribution deals with determination of mechanical properties of TiC(N) particles embedded in steel matrix by depth sensing indentation. The system belongs to a hard particle in soft matrix system. It has been shown that this technique can be applied to measure properties of the particles. The influences affecting the accuracy of measurement were described. The measured values of hardness and modulus are H_{IT} = 30 GPa and E_{IT} = 480 GPa, respectively. The physical model of particle behavior during the indentation was presented. Based on this model the influence of the particle size on measured results was determined.